Available online at www.sciencedirect.com
ScienceDirect
Food Chemistry 102 (2007) 532–541
Food Chemistry
www.elsevier.com/locate/foodchem

Some implications of nanoscience in food dispersion formulations containing phospholipids as emulsifiers

Juan M. Rodríguez Patino [a,*], Ana Lucero Caro [a], M. Rosario Rodríguez Niño [a], Alan R. Mackie [b], A. Patrick Gunning [b], Victor J. Morris [b]

[a] Departamento de Ingeniería Química, Facultad de Química, Universidad de Sevilla, cl. Prof. García González, 1, 41012 Seville, Spain
[b] Institute of Food Research, Norwich Research Park, Colney, Norwich NR4 7UA, UK

Abstract

This contribution is concerned with phospholipid films in relation to food dispersions such as emulsions and foams. Structural, morphological and surface rheological characteristics of dipalmitoyl phosphatidylcholine (DPPC) and dioleoyl phosphatidylcholine (DOPC) monolayers were determined at the air–water interface at 20 °C and at pH 5, 7, and 9, by means of surface pressure (π)–area (A) isotherms coupled with Brewster angle microscopy (BAM), atomic force microscopy (AFM) and surface dilatational and shear rheometry. From the π–A isotherms it was deduced that DPPC monolayers show structural polymorphism at the air–water interface. DOPC monolayers formed a liquid-expanded (LE) structure under all experimental conditions, a consequence of the weak molecular interactions due to the double bond in the hydrocarbon chain. Electrostatic interactions between film-forming components influence the monolayer structure. BAM and AFM images corroborate, at a microscopic and at nanoscopic level respectively, the structural polymorphism deduced from the π–A isotherm for DPPC monolayers as a function of surface pressure and the pH of the aqueous phase. However, the homogeneous morphology of DOPC monolayers at a microscopic level, as observed by BAM, shows structural heterogeneity at a nanoscopic level when observed by AFM. The relative monolayer thickness increases with surface pressure and is a maximum at the collapse point, especially for DPPC monolayers. The results confirm that the interfacial rheological characteristic measured under dilatation and shear conditions are very dependent on the structural characteristics and morphology of the phospholipids (DPPC and DOPC) monolayers.

1. Introduction

Many natural and processed foods are dispersions or have been in the dispersed state at some time during their formation. Most of these food dispersions are emulsions and foams. These dispersions include traditional food formulations, such as bakery, confectionery, meat products, ice cream, dressings and/or new formulations such as low fat and instant foods, high- or low-alcohol food formulations, and functional foods. Thus the analysis of food colloids is of practical importance (Dickinson, 1992; Friberg & Larsson, 1997; Hartel & Hasenhuette, 1997; McClements, 2005; Sjöblom, 1996).

Phospholipids, being amphiphilic and highly surface-active, can significantly influence the physical properties of technologically important emulsions and foams (Bos, Nylander, Arnebrant, & Clark, 1997). They are able to form self-assembling supramolecular structures; a key component of the ''bottom-up'' nanoscience approach for the separation of immiscible phases (Lucero et al., 2005; Lucero, 2005), vital for food dispersions and cosmetic formulations (Cevec, 1993). In addition, phospholipids possess nutritional and therapeutic properties (Golberg, 1994). This synergy between technology and physiology justifies the interest in phospholipids for the formulation of functional foods (Cevec, 1993; Golberg, 1994).

A better understanding of supramolecular structuring principles will reveal new phenomena, lead to new manufacturing processes for high-added-value food products

* Corresponding author. Tel.: +34 954 556446; fax: +34 954 556447.
E-mail address: jmrodri@us.es (J.M. Rodríguez Patino).

0308-8146/$ - see front matter © 2006 Elsevier Ltd. All rights reserved.
doi:10.1016/j.foodchem.2006.06.010

and the development of new emulsifiers (Leser, Michael, & Watzke, 2003). This means that the macroscopic characteristics of dispersions can be improved by controlling the formation of nanostructures at the interface. Such molecular-assembly (molecular engineering or nanotechnology) has been facilitated by the utilisation of traditional instruments (film balance) and new, dramatic development of advanced equipment, such as AFM, BAM, imaging ellipsometry (IE), suitable for the characterisation of the structure of such thin layered structures (Hollars & Dunn, 1998; Mackie, Gunning, Wilde, & Morris, 2000; Morris, Kirby, & Gunning, 1999). This represents one way in which nanoscience can lead to new, nanotechnological fabrication of complex food colloids. However, since phospholipids can be present at interfaces with different net charges, depending on the pH, an analysis of the effect of the pH of the aqueous phase on structure formation will give new insights into the importance of such electrostatic interactions on self-assembly in spread phospholipid monolayers, a key component of the molecular engineering approach.

This contribution is concerned with the analysis of the structures formed by the phospholipids (DPPC and DOPC) at the air–water interface, using the complementary techniques of the film balance, BAM, AFM, and surface rheology. Phospholipids show a strong tendency to adsorb at fluid interfaces and, for this reason, they find an important use in the manufacture of stable traditional and new food dispersions (chocolate, margarine, spreads, mayonnaise, cereal-based products – i.e. bread, cakes, and other bakery products –, low-fat products, products for infant nutrition, functional foods, etc.). The article demonstrates (i) the effect of the type of phospholipid on the interfacial structure and morphology (self-assembly), (ii) the role of electrostatic interactions between phospholipids on interfacial self-assembly, and (iii) the dilational and shear phenomena at fluid interfaces. Finally, the role of emulsifiers at fluid interfaces is discussed with particular reference to their properties at the nano- and/or mesoscale in the formation and stability at the micro- and macroscopic scale of model food emulsions and foams.

2. Materials and methods

2.1. Materials

Surface films of the phospholipids DPPC and DOPC (Sigma, 99%) were formed by spreading the solution at the interface, using chloroform/ethanol (4:1, v:v) as a spreading solvent. Analytical grade chloroform (Sigma, 99%) and ethanol (Merck, >99.8%) were used without further purification. The subphase pH was adjusted using acetic acid/sodium acetate to achieve pH 5, and a commercial buffer, called *trizma* ($(CH_2OH)_3CNH_2$/$(CH_2OH)_3$-CNH_3Cl), for obtain pH 7 and 9. All of these products were supplied by Sigma (>99.5%).

2.2. Surface film balance

For a fundamental understanding of the role of emulsifiers in the stabilization of food dispersions, it is essential to obtain information on their packing at the interface. Such information can be obtained through surface pressure (π) versus average area per molecule (A) from investigation of spread monolayers at the air–water interface. Measurements of the π–A isotherms were performed on fully automated Langmuir- and Wilhelmy-type film balances, as described elsewhere (Rodríguez Patino, Carrera, & Rodríguez Niño, 1999a; Rodríguez Patino, Carrera, & Rodríguez Niño, 1999b). Each π–A isotherm was measured five times. The reproducibility of the results was better than ± 0.5 mN/m for measurements of π and ± 0.05 m^2/mg for measurements of A.

2.3. Brewster angle microscopy (BAM)

The advent of high-resolution Brewster angle microscopy (BAM) has made it possible to directly visualize interfacial films with a reasonable spatial resolution (ca. 2 μm). The evolution with the surface pressure of BAM images and relative reflectivity (or relative film thickness) gives complementary information, at a microscopic level, on the structural characteristics and interactions of spread emulsifier monolayers (Rodríguez Patino et al., 1999a, 1999b). Microscopic observations of the interfacial monolayer and measurements of the relative reflectivity (I) of the film structure were made using a commercial Brewster angle microscope (BAM), BAM2, manufactured by NFT (Göttingen, Germany) as described elsewhere (Rodríguez Patino et al., 1999a, 1999b). To measure the relative thickness of the film a previous camera calibration is necessary in order to determine the relationship between the gray level (GL) and the reflectivity (I). The reflectivity at each point in the BAM image depends on the local thickness and film optical properties. These parameters can be measured by determining the light intensity at the camera and analyzing the polarization state of the reflected light. At Brewster angle $I = C \cdot \delta^2$, where C is a constant and δ is the film thickness (Rodríguez Patino et al., 1999a, 1999b). The imaging conditions were adjusted in order to optimise both the image quality and the quantitative measurement of reflectivity.

2.4. Atomic force microscopy (AFM)

Atomic force microscopy is a powerful method for imaging surface detail on flat substrates at molecular resolution. The power of the technique is that it can impart interfacial thickness information with extremely high spatial resolution (Mackie, Gunning, Wilde, & Morris, 1999). The atomic force microscope used in this study was manufactured by East Coast Scientific Limited (Cambridge, UK). The cantilevers were the short, narrow variety from the 'nanoprobe' range with quoted spring constants

of 0.38 N/m. In order to obtain images of the DPPC and DOPC monolayers the interfacial structures were sampled by the Langmuir–Blodgett (LB) method and the LB films deposited onto hydrophilic, freshly cleaved mica substrates, in the manner described elsewhere (Mackie et al., 1999). Images were obtained in the dc contact mode in air.

2.5. Surface dilatational rheology

Surface dilatational rheological parameters (the surface dilatational modulus (E), its storage (Ed) and loss (Ev) components and the phase angle, ϕ) of spread monolayers at the air–water interface were measured using a modified Wilhelmy-type film balance (KSV 3000) (Rodríguez Patino, Rodríguez Niño, Carrera, & Cejudo, 2001). In this method the surface is subjected to small periodic sinusoidal compressions and expansions by means of two oscillating barriers at a given frequency (ω) and amplitude ($\Delta A/A$) and the response of the surface pressure is monitored (π). Surface pressure was directly measured by means of two roughened platinum plates situated on the surface between the two barriers. The dilatational modulus – a measure of the total unit material dilatational resistance to deformation (elastic + viscous) – is a complex quantity and is composed of real and imaginary parts, $E = \mathrm{Ed} + \mathrm{iEv}$. The reproducibility of the measured surface dilatational modulus values (for two measurements) was better than 5%. The surface dilatational viscoelasticity of food emulsifiers is relevant for the stability of the emulsion or foam in the production stage. The surface rheology of emulsifiers at the air–water interface is of interest not only due to its importance in relation to dispersion stability, but also because of its extreme sensitivity to the nature of intermolecular interactions at the interface.

2.6. Surface shear rheology

Measurements of surface shear rheology were made using a commercial automatic oscillatory ring apparatus (Camtel CIR 100, Camtel Ltd., Royston, UK) as described previously (Warburton, 1993). The oscillation resonance frequency was 3 Hz, and the strain amplitude was set to 5×10^{-3} rad. The storage (G') and loss (G'') components of the shear moduli were calculated from the applied forces required to maintain the resonance frequency and amplitude (normalized resonance mode). Surface shear viscosity may contribute appreciably to the long-term stability of dispersed systems.

3. Results and discussion

3.1. Structural characteristics of phospholipid films

The thermodynamic behaviour of spread films at the air–water interface are expressed by the π–A isotherms, obtained in a film balance. From the nature of the π–A isotherm, different structures can be deduced for phospholipid monolayers, as a function of pH, temperature, and the surface density or surface pressure. Results derived from π–A isotherms at pH 5, 7, and 9 (Fig. 1) in the Langmuir- and Wilhelmy-type troughs are similar.

The different structures deduced for the DPPC monolayers as a function of pH and surface pressure are shown in Fig. 1A. At pH 7 the π–A isotherm shows three distinct regions: a liquid-expanded (LE) phase (at $\pi < 5.5$–9.5 mN/m), a first-order phase transition – the intermediate region of lower slope – between liquid-condensed (LC) and liquid-expanded structures (at $9.5 < \pi < 30$ mN/m), the liquid-condensed structure (at $\pi > 30$ mN/m) and finally monolayer collapse at a surface pressure of about 55 mN/m. These results are in agreement with those observed for the same phospholipid at neutral pH (Matsumoto, Tsujii, Nakamura, & Yoshimoto, 1996; McConlogue, Malamud, & Vanderlick, 1998; Miñones, Rodríguez Patino, Conde, Carrera, & Seoane, 2002). The pH of the aqueous phase also has an effect on the structural characteristics of DPPC.

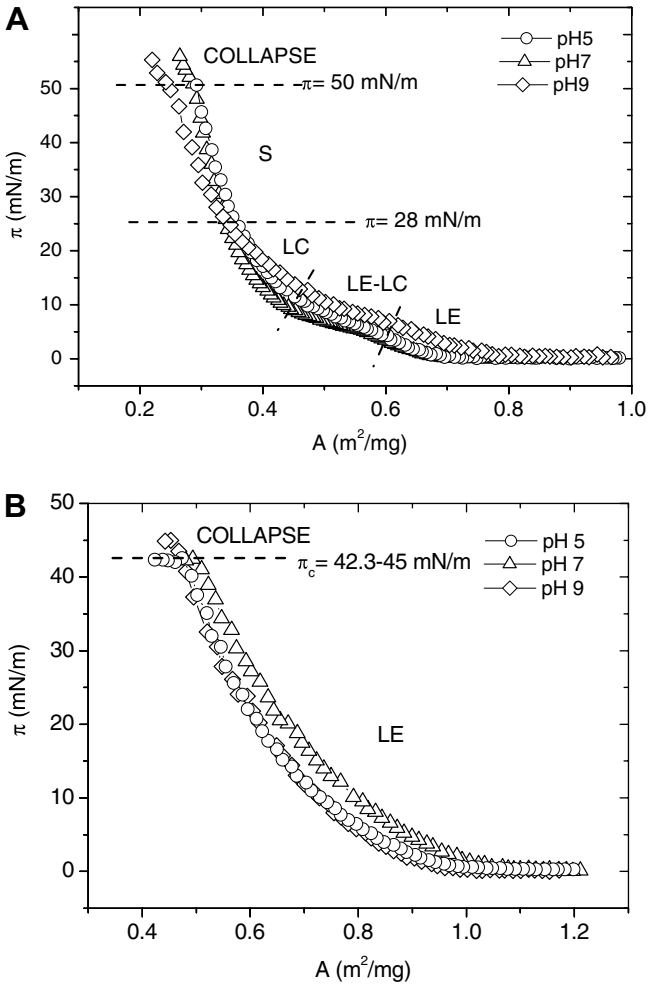

Fig. 1. Surface pressure (π)–area (A) isotherms for (A) DPPC and (B) DOPC monolayers spread at the air–water interface, measured as a function of the pH of the aqueous phase at 20 °C and an ionic strength 0.05 M. The symbols S, LC and LE denote solid, liquid-condensed and liquid-expanded phases.

In fact, π at the beginning of the first-order phase transition between the LE and LC phases was found to be higher at pH 9 than at pH 7 or 5.

DOPC monolayers (Fig. 1B) formed a liquid-expanded (LE) structure under all experimental conditions, because the double bond in the hydrocarbon chain weakened molecular interactions or packing of the hydrocarbon chains. DOPC monolayers were found to be more expanded at neutral pH.

Both DPPC and DOPC formed 2D-foams at low surface pressures and they were also found to form interfacial soluble vesicles at high surface pressures. It is important to note that the presence of a double bond in the DOPC molecule also produced a shift of the π–A isotherms towards higher molecular areas, when compared with the DPPC monolayers, due to the more expanded structure within the DOPC monolayers.

3.2. Morphological characteristics of phospholipid films

By combining the surface pressure measurements with direct microscopic visualization of the monolayer by BAM (Fig. 2) and by AFM visualization of monolayers transferred onto solid supports (data not shown), a range of phospholipid microdomains were characterized (Fig. 3). BAM and AFM corroborated the structural polymorphisms deduced from the π–A isotherms for DPPC. At low surface pressures the BAM images showed the existence of a homogeneous film of the LE structure. Once the plateau surface pressure is attained, small, irregular LC domains with 4–6 lobes, that are brighter than the surrounding area, are formed. In the phase transition region these LC domains increase in size. The lobed-like shape of the DPPC LC domains was also observed by Miñones Jr. et al. (2002), and is attributed to the chirality of the DPPC molecules (Weis & Connell, 1984). Once the LE–LC transition region is exceeded, the domains merge together as a result of compression, and their lobed structure slowly blurs until it disappears completely just before the monolayer collapse point, giving a homogenous image. At the end of the compression, the monolayer collapse is evidenced by the formation of bright fractures.

BAM images confirm that only the homogeneous liquid-expanded phase is present during the compression of a DOPC monolayer (Fig. 2). From the observations with BAM, together with the data obtained from the film balance, no fractures were observed after the DOPC collapse. This is because the collapse of the DOPC monolayer occurs through the formation of lenses. However, DOPC monolayers, which appeared to be homogeneous at the microscopic level when visualized using BAM, showed heterogeneity at the nanoscopic level when observed using AFM, as will be discussed later.

3.3. Memory effects on the monolayer structure and morphology

Contrary to the behaviour of polar lipids (Rodríguez Niño, Rodríguez Patino, Carrera, Cejudo, & Navarro, 2003), phospholipids (Miñones Jr. et al., 2002), and other surfactants containing a double hydrocarbon chain (Gonçalves da Silva, Romao, Lucero, & Rodríguez Patino, 2004) show memory effects which are more evident during the first expansion after the compression of the monolayer up to the collapse point. For instance, during the first expansion of a DPPC monolayer, after compression up to the monolayer collapse point (Fig. 3), the characteristic topography of a collapsed DPPC monolayer (Fig. 3Aa), which is present during the monolayer expansion (Fig. 3Ab) were visualized. At the lower surface pressures

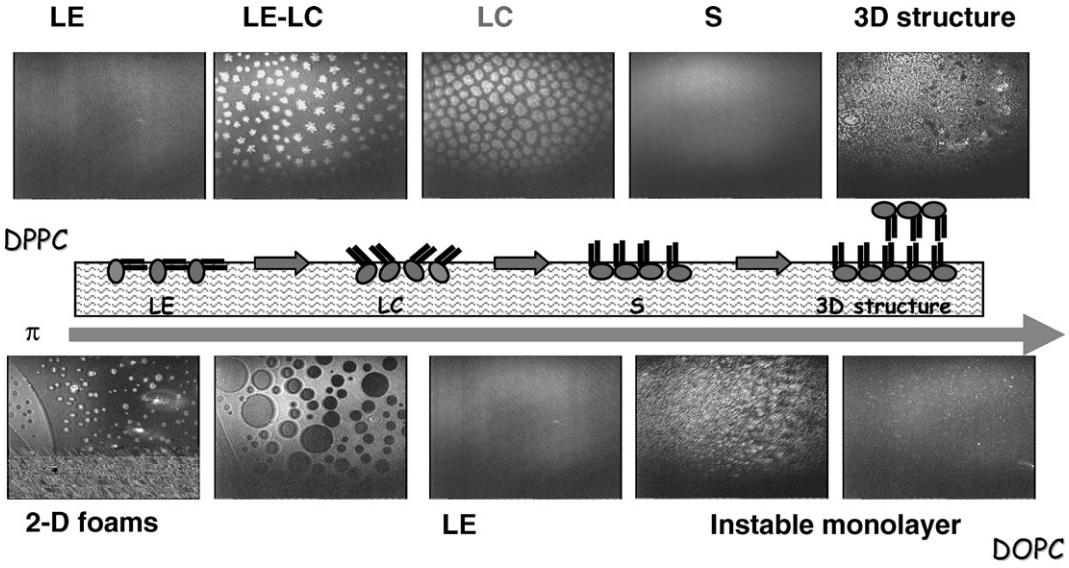

Fig. 2. Visualization of DPPC and DOPC monolayers at the air–water interface by BAM. Data was acquired at a temperature 20 °C and pH 7. The images sizes are 470 × 600 μm. The images illustrate the different types of structures formed at the interface. The cartoon is a schematic picture of the different phases formed by the DPPC.

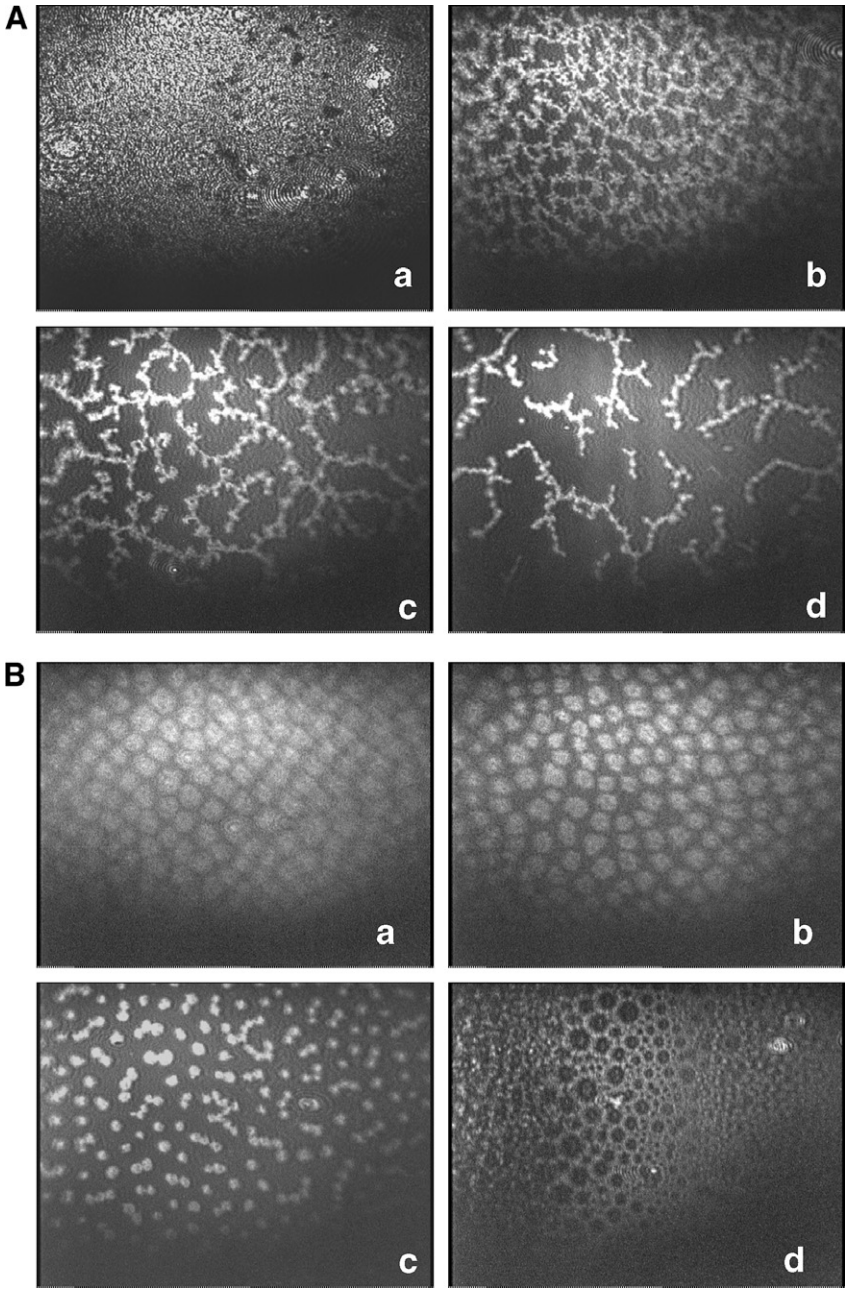

Fig. 3. Memory effects in DPPC monolayers as visualized by BAM. The image sizes are 470 × 600 μm. (A) Structures seen on the first expansion after collapse of the DPPC monolayers at various surface pressures: (a) 11 mN/m, (b) 7.8 mN/m, (c) 6.9 mN/m and (d) 5.6 mN/m. (B) Structures seen on subsequent expansion of DPPC monolayers as a function of surface pressure: (a) 16.4 mN/m, (b) 11.7 mN/m, (c) 6.5 mN/m, and (d) 0.3 mN/m. Temperature 20 °C, pH 7.

a pearl-pendant-like morphology is observed (Fig. 3Ac) as a result of attractions and repulsions between DPPC domains. The LC domains organize as fractal-like structures instead of the random distribution of domains observed during compression. The density of fractal-like structures decreases during the expansion (Fig. 3Ad), and a homogeneous black image is recovered at the lowest surface pressure (image not shown). However, as the DPPC monolayer has been compressed previously the topography during the expansion is similar to that during the compression but the reverse evolution (Fig. 3B). Thus, although the π–A isotherms are reproducible after successive compression–expansion cycles, at a microscopic level there exists differences in the monolayer morphology because of the self-association of DPPC molecules during compression and specially after the monolayer collapse. These results demonstrate that the morphology of the DPPC monolayers depends on the history of the monolayer.

3.4. Observing monolayer structure at different levels of magnification

BAM and AFM can be utilised to visualize the monolayer structure in the transition between the LE and LC

phases at different level of magnification (Fig. 4). It can be seen that although BAM and AFM use different physical principles, namely reflectivity in the case of BAM and topography in the case of AFM, the monolayer structures observed by these two techniques are essentially similar and complementary (Mackie, Gunning, Ridout, Wilde, & Rodríguez Patino, 2001). BAM provides direct, *in situ* and direct observation of the monolayer structure but with limited resolution. The AFM observations can yield higher resolution, but the monolayer structure has to be sampled and imaged whilst supported on a solid hydrophilic mica substrate. The correspondence between the topographic structural information obtained from these two methods confirms that the transfer of the monolayer onto a solid support does not affect the molecular organization within the monolayer. AFM is a powerful method for imaging surface detail on supported, flat substrates at nanoscopic resolution: in addition the AFM provides direct information on the height or topography of the structure. From these results it can concluded that the phenomenological changes observed by BAM and AFM in DPPC monolayers as a function of pH are essentially the same when viewed at equivalent levels of magnification. However, the AFM data reveals previously unexpected heterogeneity within the domains and at the surfaces of the domain structures (Fig. 4). The topographic images suggest the presence of small, but numerous holes in the interior of the domains (possibly LE regions) and ragged surface protrusions at the domain boundaries.

Although BAM data suggests that the DOPC layers are homogeneous during compression, the new AFM data reveals levels of heterogeneity at a nanoscopic level (Fig. 5). In the AFM images at low surface pressures (at 4 mN/m) the interfacial structure appears to be homogeneous (Fig. 5a). However, this sample has been scanned at 50 μm which is close to the maximum scan range of the AFM scanner (60 μm). Thus the image will show some eye-balling and it may not be possible to detect small variations in height within the image. The image shown in Fig. 5a does show some evidence of a mottled appearance and this is confirmed in scans made at lower scan sizes (Fig. 5b and c). Such fluctuations in height may indicate bilayer formation within certain regions of the interfacial layer. At higher surface pressures (>14 mN/m) the AFM images revealed the presence of small bright nucleus (Figs. 5d and e), which can be attributed to the formation of structures with large heights. In the images shown in Fig. 5d and e the large objects dominate the contrast in the images and it would be difficult to identify any fine structure within the interfacial layer surrounding these objects. By collecting images in the apparently homogeneous region surrounding these large objects (Fig. 5a and d) it can be seen that at these higher surface pressures the interfacial layers are also mottled in appearance. This would seem to suggest that the interfacial layers can form multilayers or vesicles and this phenomenon demonstrate the tendency of phospholipids to form interfacial vesicles.

3.5. The effect of electrostatic interactions on the structural characteristics and topography of the monolayer

From the π–A isotherms (Fig. 1A) we can conclude that the monolayer structures of DPPC are practically the same

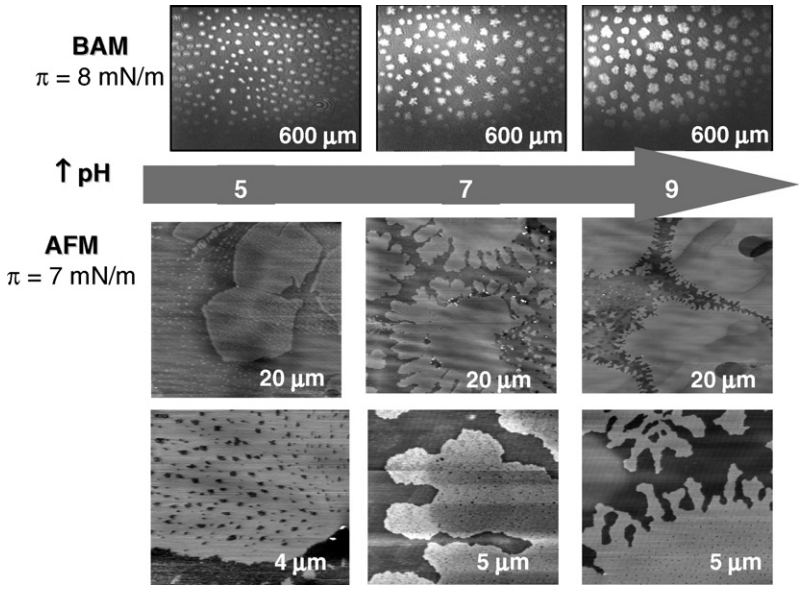

Fig. 4. Visualization of DPPC monolayer structures formed at the air–water interface by BAM and AFM at a temperature of 20 °C. The BAM data show images collected at a surface pressure of 8 mN/m. The BAM image sizes are 470 × 600 μm. The AFM data was obtained at a surface pressure of 7 mN/m. The total AFM image size is shown on the images: 20 μm means an image size of 20 × 20 μm. The BAM and AFM data show images collected at different pH values: pH 5, 7 and 9.

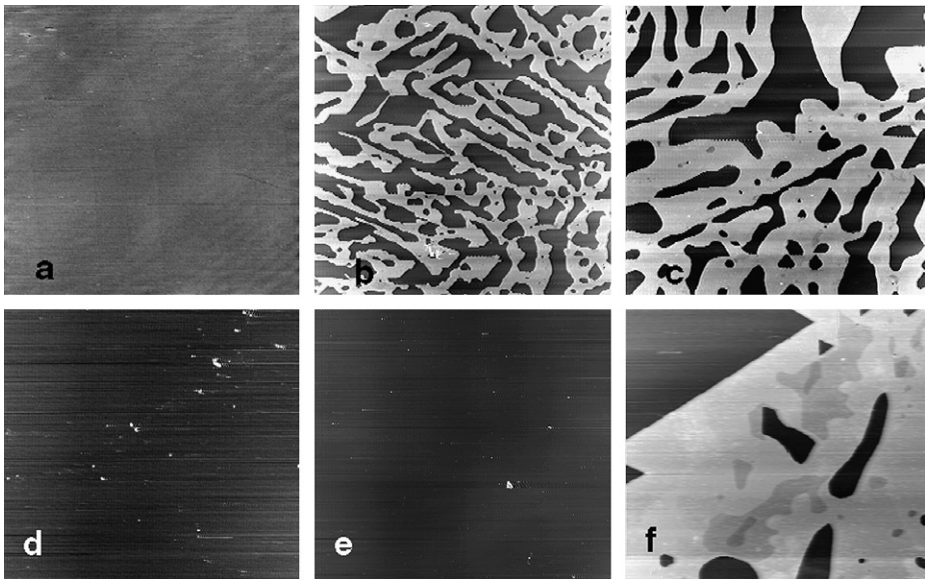

Fig. 5. AFM images of the morphology of DOPC monolayers at a surface pressure of 4 mN/m. The interfaces were sampled at the air–water interface and transferred onto mica substrates. Image sizes are (a) 50×50 μm, (b) 20×20 μm, and (c) 10×10 μm. AFM images of the morphology of DOPC monolayer at 14 mN/m after transfer onto mica substrates. Image sizes are (d) 20×20 μm, (e) 10×10 μm, and (f) 4×4 μm.

at pH 5 and 7, but that a more expanded structure was observed in the monolayer at pH 9. The surface pressure at the transition between LE and LC structures also decreases at pH 9. These phenomena can be explained by the effect of electrostatic repulsions between head group of DPPC molecules at pH 9 (Lucero et al., 2005). In contrast to what has been observed for the DPPC layers, similar changes in pH do not seem to have similar effects on the structure of DOPC monolayers (Fig. 1B). Thus, the structure of DOPC monolayers is dominated by the orientation of the hydrocarbon chains, relegating the effect of the polarity of the head group as a function of pH to having a minor effect on the film structure (Lucero et al., 2005).

The pH of the aqueous phase has a significant effect on the topography of the DPPC monolayers (Fig. 4). Electrostatic interactions clearly play a role in the self-assembly of domains within DPPC layers as observed in the BAM images. At pH 5, the DPPC domains are small and compact in shape. As the pH increases the domains increase in size. In addition the shape of the domains changes with the domains becoming clearly dendrite-like in appearance. This is presumably because increasing the boundary length minimises the effects of repulsive interactions between DPPC molecules within the domain. The higher size in DPPC domains were observed at pH 9 because these domains are partially submerged into the aqueous phase sublayer in order to reduce the repulsions between DPPC polar groups. The fact that these domains are not clearly separated confirms these phenomena. In summary, the structure of LC domains within DPPC monolayers depends on the pH of the aqueous phase pH because of the interplay between dipole–dipole interactions and the lineal tension as a function of the pH.

3.6. Monolayer thickness

In addition to direct observation of the monolayer by BAM or AFM, the measured reflectivity (I) or thickness of the monolayer gives complementary information at a microscopic or nanoscopic level, respectively, on the structural characteristics of the emulsifiers during monolayer compression (Horne & Rodríguez Patino, 2003; Rodríguez Patino et al., 1999b).

From the reflectivity (I)–π curve it is possible to identify the liquid-expanded, liquid-condensed, solid structural regions and, finally collapse at the highest surface pressure (Fig. 6A) of the DPPC monolayers. In the LE–LC region the reflectivity increases with increasing surface pressure because the polar groups, which are originally submerged within the aqueous subphase, emerge at the interface during the compression. The change in the penetration of the polar groups into the subphase is coincident with the main transition between the LE and LC structures at the interface (i.e., with the monolayer structuring). The noise in the reflectivity data which will arise due to variations in the thickness of the films is due to the presence of LC domains (with high reflectivity) distributed within the homogenous LE phase (with low reflectivity). In the LC region the thickness increases with increasing surface pressure because the hydrocarbon chains acquire a lower inclination with respect to the interfacial plane. At higher surface pressures the thickness becomes constant; coinciding with the formation of the solid structure within the monolayer. Thus, the inflection in the π–A isotherm at 28 mN/m (Fig. 1A) is due to a change in the orientation of the hydrocarbon chains towards a vertical position in the solid region. Finally, reflectivity changes at the highest surface pressure are due to collapse of the monolayer.

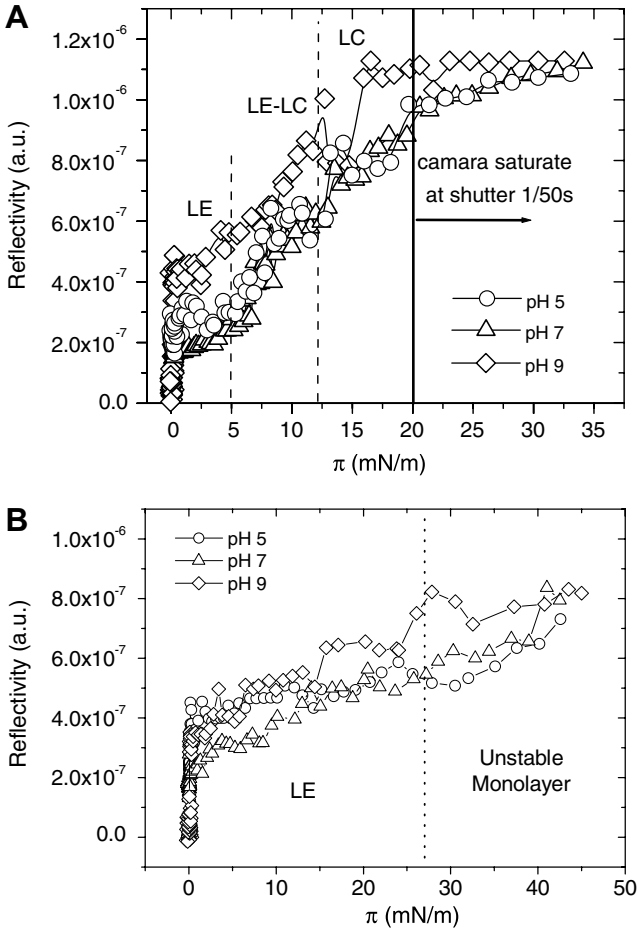

Fig. 6. Variation of the surface reflectivity of BAM images with surface pressure for (A) DPPC and (B) DOPC monolayers spread at the air–water interface. The data was collected at a shutter speed of 1/50 s. Data was obtained for the first compression of the monolayer. Temperature 20 °C, pH 7 and ionic strength 0.05 M.

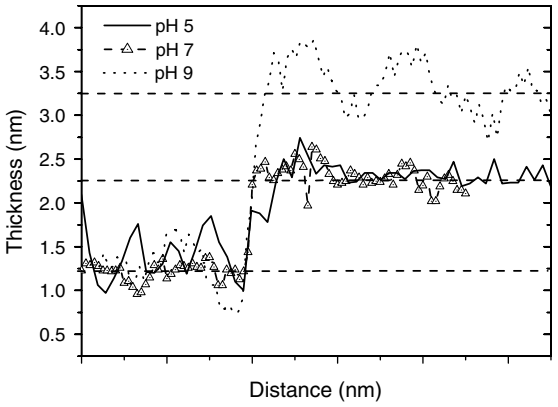

Fig. 7. Height profiles of DPPC monolayers showing the height change at the boundary of an LC domain. The monolayers were spread at the air–water interface. Samples were collected at a surface pressure of 6.7 mN/m and transferred to mica substrates. Data was obtained at 20 °C, at an ionic strength of 0.05 M and as function of pH.

At pH 9 the monolayer thickness determined from the AFM data is 1.44 times higher in the LE region and 1.28 times higher in the solid region as compared with those at pH 5 and 7 (Fig. 7). The increase in the monolayer reflectivity (Fig. 6) and thickness (Fig. 7) with pH can be attribute to a higher affinity between water molecules and polar group as DPPC molecules are ionised on a basic aqueous phase. That is, the higher thickness of DPPC monolayer at pH 9 may be due that under these conditions the DPPC polar group is partially submerge into the aqueous phase.

In contrast with observations for the DPPC layers, the reflectivity–π curves for DOPC monolayers (Fig. 6B) are consistent with the presence of only the LE structure during compression of the monolayer up to the collapse point at the highest surface pressure. Finally, the reflectivity, or the film thickness, during compression of the monolayer and especially at the collapse point, is lower for the DOPC monolayers than for the DPPC monolayers. The presence of an unsaturated double bond causes an addition tilt in the hydrocarbon chain for the DOPC molecules, and this tilt is not changed significantly during the compression of the DOPC monolayer. The increase in the DOPC monolayer reflectivity (thickness) at the highest surface pressure is attributed to the nucleation of interfacial lenses or vesicles.

3.7. Viscoelastic properties of phospholipid monolayers

The structural characteristics of phospholipid monolayers influence their viscoelastic properties as measured under dilatational and shear conditions. Surface rheology is a very sensitive tool for the characterisation of structural polymorphism in spread monolayers (Horne & Rodríguez Patino, 2003; Rodríguez Niño et al., 2003).

Fig. 8 show that a common feature of the surface pressure dependence of dilatational modulus (E) for the DPPC and DOPC monolayers is that E increases with increasing π up to the collapse point. This increase is a result of the increase in the interactions between the molecules within the monolayer, as deduced from the measurements of monolayer reflectivity (Fig. 6) and thickness (Fig. 7). However, for the more condensed DPPC monolayer (Fig. 8A) this increase is higher than that observed for the more expanded DOPC monolayer (Fig. 8B). In summary, the I–π and E–π curves reflect the behaviour illustrated by the surface equation of state of the spread emulsifier at the air–water interface (Horne & Rodríguez Patino, 2003; Rodríguez Niño et al., 2003). However, the measurements of the surface dilatational rheology are clearly not very sensitive to electrostatic interactions between DPPC molecules within the monolayers, because changing the pH of the aqueous phase does not have a significant effect on the magnitude of the surface dilatational modulus (Fig. 8A).

However, measurements of surface shear rheology for DPPC monolayers are clearly sensitive to both the structure of the monolayer and the nature of the electrostatic interactions between molecules within the monolayer (Fig. 9). It can be seen that both the elastic (G') and viscous

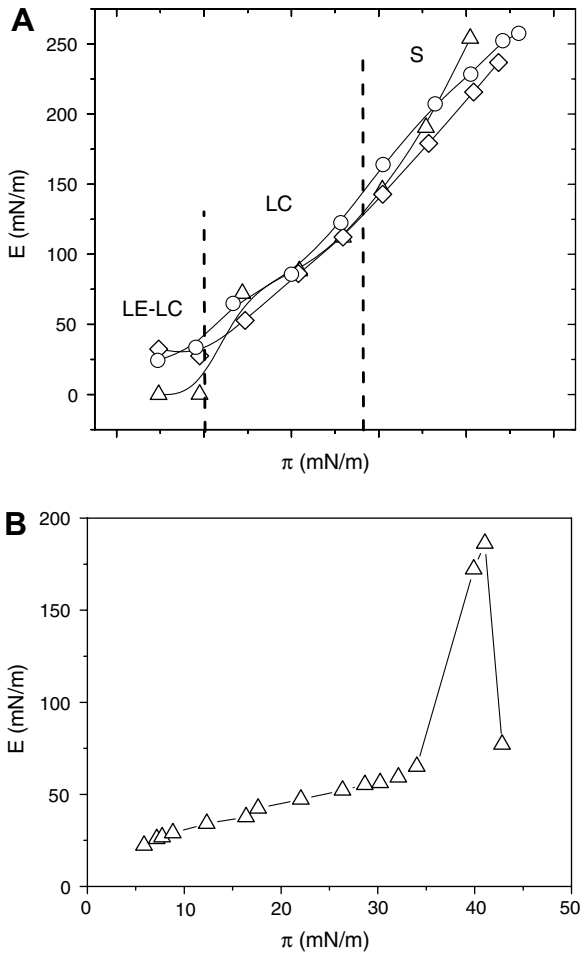

Fig. 8. The dependence of the surface dilatational modulus (E) on surface pressure for (A) DPPC and (B) DOPC monolayers. The monolayers were spread at the air–water interface at 20 °C and ionic strength 0.05 M. The frequency of deformation is 50 mHz at an amplitude of deformation of 5%. Aqueous phase pH values are (○) 5, (△) 7, and (◇) 9.

(η_s) components of the surface shear modulus increase with the increasing surface density. In addition, the both G' and G'' also increase as the pH of the aqueous phase decreases. Previously it has been suggested that the repulsive interactions between DPPC polar groups at pH 9 produces a lower packing of the monolayer and larger domains, as observed in by BAM (Fig. 4). It seems reasonable to suppose that these phenomenon are responsible for the values of G' and η_s measured at pH 9 under shear conditions. The surface shear rheology is sensitive to electrostatic interactions between DPPC molecules within the monolayers.

In summary, the results with phospholipids monolayers confirm (Horne & Rodríguez Patino, 2003; Rodríguez Niño et al., 2003) that the dilatational and shear modulus are not only determined by the interactions between spread molecules which determine the surface pressure or surface density, but on the detailed morphological of the structures formed at the interface.

3.8. Implications of the effects of nanostructures on model food dispersion formulations

In a recent contribution (Carrera & Rodríguez Patino, 2005) the interfacial, foaming and emulsifying characteristics of a typical milk protein (sodium caseinate) were analysed as a function of the protein concentration in aqueous solution. It was observed that there are close relationships between foaming behaviour (power of foaming, foam capacity, foam density, and foam conductivity) and the rate of diffusion of caseinate to the air–water interface. The rate of diffusion is a maximum when the film is saturated by the protein, at a surface density that is close to that of the collapse pressure of the protein monolayer. The foam stability, as monitored by the quantified relaxation time for drainage and disproportionation/collapse, was found to show a linear correlation with the equilibrium surface pressure (π_e) of the aqueous caseinate solutions. The π_e value is the maximum surface pressure to which a monolayer can be compressed before the collapse. At surface pressures lower than that required for monolayer saturation the foaming was zero. The emulsifying capacity, as quantified by measurements of the droplet size and the specific surface area, was also correlated with the protein concentration in solution (the surface pressure at equilibrium).

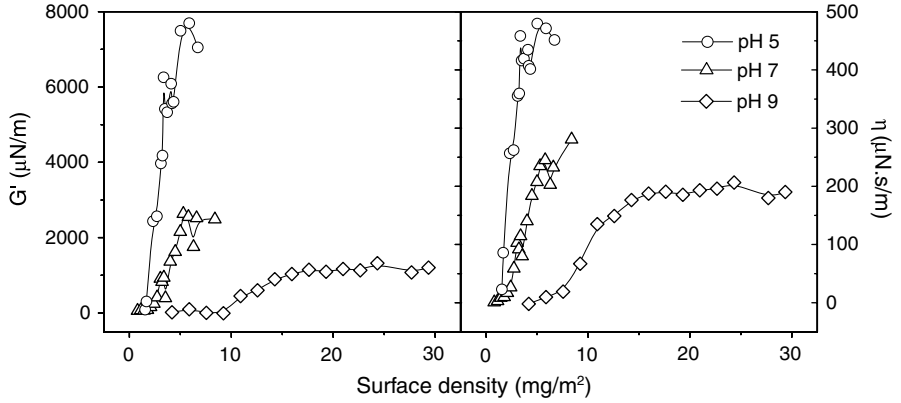

Fig. 9. The effect of surface density on the shear rheology (storage modulus G' and the viscosity, η_S calculated from the loss component components G'') for DPPC monolayers. The monolayers were spread at the air–water interface at 20 °C and an ionic strength of 0.05 M. Aqueous phase pH values are (○) 5, (△) 7, and (◇) 9.

Coalescence was observed only at lower caseinate concentrations in solution where a diluted monolayer is formed at the interface. When a coherent protein layer (multilayer) saturates the interface at higher protein concentrations in solution, the instability of the emulsion is due to flocculation and/or creaming. Coalescence and creaming rates correlate well with the protein concentration in solution and hence with the surface pressure and/or surface dilatational modulus. This results demonstrate that macroscopic characteristics of foams or emulsions, generated using aqueous emulsifier solutions, depends on the microscopic and nanoscopic structural, topographical and surface rheological characteristics of the interfacial films formed by the emulsifiers at fluid interfaces.

4. Conclusions

The structure, morphology, film thickness and surface dilational and shear rheology of DPPC and DOPC monolayers were determined at the air–water interface using surface pressure (π)–area (A) isotherms, Brewster angle microscopy, atomic force microscopy, and surface rheology. DPPC monolayers showed a structural polymorphism dependent on π, displaying film anisotropy and heterogeneous domain structures. DOPC monolayers formed a liquid-expanded (LE) structure under all experimental conditions. Both BAM and AFM corroborated the structural polymorphisms deduced from the π–A isotherms obtained for DPPC samples. The results demonstrate that the structure, morphology and surface rheology of phospholipid monolayers are very sensitive to the nature of the hydrocarbon chain and the pH of the aqueous phase.

Acknowledgements

The authors acknowledge the support of CICYT thought the grants AGL2001-3843-C02-01 and AGL2004-01306/ALI. Research at IFR is funded through the core BBSRC grant to the Institute.

References

Bos, M., Nylander, T., Arnebrant, T., & Clark, D. C. (1997). In G. L. Hasenhuette & R. W. Hartel (Eds.), *Food emulsions and their applications* (p. 95). New York: Chapman and Hall.

Carrera, C., & Rodríguez Patino, J. M. (2005). Interfacial, foaming and emulsifying characteristics of sodium caseinate as influenced by protein concentration in solution. *Food Hydrocolloids, 19*, 407–416.

Cevec, G. (1993). *Phospholipids handbook*. New York: Marcel Dekker.

Dickinson, E. (1992). *An introduction to food colloids*. Oxford, UK: Oxford University Press.

Friberg, S. E., & Larsson, K. (1997). *Food emulsions* (3rd ed.). New York: Marcel Dekker.

Golberg, G. (1994). *Functional foods, designer foods, pharmafoods, nutraceuticals*. New York: Chapman Hall.

Gonçalves da Silva, A. M., Romao, R. S., Lucero, A., & Rodríguez Patino, J. M. (2004). Memory effects on the interfacial characteristics of dioctadecyldimethylammonium bromide monolayers at the air–water interface. *Journal of Colloid and Interface Science, 270*, 417–425.

Hartel, R., & Hasenhuette, G. R. (1997). *Food emulsifiers and their applications*. New York: Chapman and Hall.

Hollars, C. W., & Dunn, R. C. (1998). Submicron structure in L-α-dipalmmitoyl-phoshsphatidyl-choline monolayers and bilayers probed with confocal, atomic force, and near-field microscopy. *Biophysical Journal, 75*, 342–353.

Horne, D. S., & Rodríguez Patino, J. M. (2003). In M. Malmsten (Ed.), *Biopolymers at interfaces* (pp. 857). New York: Marcel Dekker.

Leser, M. E., Michael, M., & Watzke, H. J. (2003). Food goes nano: new horizons for food structure research. In E. Dickinson & T. van Vliet (Eds.), *Food colloids: Biopolymers and materials* (pp. 3–13). Cambridge, U.K.: Royal Society Chemistry.

Lucero, A., Rodríguez Niño, Ma. R., Carrera, C., Gunning, A. P., Mackie, A. R., & Rodríguez Patino, J. M. (2005). Displacement of β-casein from the air–water interface by phospholipids. In E. Dickinson (Ed.), *Food colloids: Interactions, microstructure and processing* (pp. 160–175). Cambridge: The Royal Society of Chemistry.

Lucero, C. (2005). Propiedades Interfaciales de Emulsionantes Alimentarios: Fosfolípidos y Proteínas. Ph.D. Thesis, University of Seville, Seville, Spain.

Mackie, A. R., Gunning, A. P., Ridout, M. J., Wilde, P. J., & Rodríguez Patino, J. M. (2001). In situ measurement of the displacement of protein films from the air/water interface by surfactants. *Biomacromolecules, 2*, 1001–1006.

Mackie, A. R., Gunning, A. P., Wilde, P. J., & Morris, V. J. (1999). Orogenic displacement of β-lactoglobulin from the air/water interface by sodium dodecyl sulphate. *Journal of Colloid and Interface Science, 210*, 157–166.

Mackie, A. R., Gunning, A. P., Wilde, P. J., & Morris, V. J. (2000). Orogenic displacement of protein from the oil–water interface. *Langmuir, 16*, 2242–2247.

Matsumoto, M., Tsujii, Y., Nakamura, K. I., & Yoshimoto, T. (1996). A trough with radial compression for studies of monolayers and fabrication of Langmuir–Blodgett films. *Thin Solid Films, 280*, 238–243.

McConlogue, C. W., Malamud, D., & Vanderlick, T. K. (1998). Interaction of DPPC monolayers with soluble surfactants: electrostatic effects of membrane perturbants. *Biochimica et Biophysica Acta–Biomembranes, 1372*, 124–134.

McClements, D. J. (2005). *Food emulsions: Principles, practice and techniques* (2nd ed.). Boca Raton, FL: CRC Press.

Miñones, J., Jr., Rodríguez Patino, J. M., Conde, O., Carrera, C., & Seoane, J. R. (2002). The effect of polar groups on structural characteristics of phospholipid monolayers at the air–water interface. *Colloids & Surfaces A: Physicochemical and Engineering Aspects, 203*, 273–286.

Morris, V. J., Kirby, A. R., & Gunning, A. P. (1999). *Atomic force microscopy for biologists*. London, UK: Imperial College Press.

Rodríguez Niño, M. R., Rodríguez Patino, J. M., Carrera, C., Cejudo, M., & Navarro, J. M. (2003). Physicochemical characteristics of food lipids and proteins at fluid–fluid interfaces. *Chemical Engineering Communications, 190*, 15–47.

Rodríguez Patino, J. M., Carrera, C., & Rodríguez Niño, Ma. R. (1999a). Morphological and structural characteristics of monoglyceride monolayers at the air–water interface by Brewster angle microscopy. *Langmuir, 15*, 2484–2492.

Rodríguez Patino, J. M., Carrera, C., & Rodríguez Niño, Ma. R. (1999b). Structural and morphological characteristics of β-casein monolayers at the air–water interface by Brewster angle microscopy. *Food Hydrocolloids, 13*, 401–408.

Rodríguez Patino, J. M., Rodríguez Niño, M. R., Carrera, C., & Cejudo, M. (2001). Structural-dilatational characteristics relationships of monoglyceride monolayers at the air–water interface. *Langmuir, 17*, 4003–4013.

Sjöblom, J. (1996). *Emulsions and emulsion stability*. New York: Marcel Dekker.

Warburton, B. (1993). Surface rheology. In A. A. Collyers (Ed.), *Technologies in rheological measurements* (pp. 55–97). London: Chapman & Hall.

Weis, R. M., & Connell, H. M. (1984). Two-dimensional chiral crystals of phospholipid. *Nature, 310*, 47–51.